Cornell University

Magnetomechanics Research

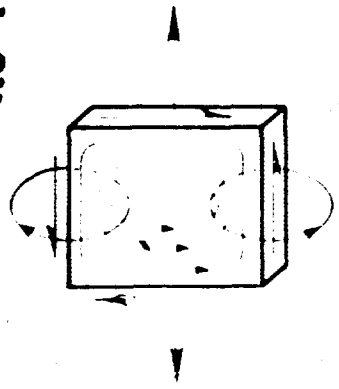

Departments of Theoretical & Applied Mechanics and Structural Engineering

EDDY CURRENT FLOWS AROUND CRACKS IN THIN PLATES FOR NONDESTRUCTIVE TESTING[1]

S. Mukherjee[2]

M.A. Morjaria[3]

and

F.C. Moon[4]

Department of Theoretical and Applied Mechanics
Cornell University
Ithaca, NY 14850

March 1981

(1) Sponsored in part by the U.S. Office of Naval Research under Contract No. N00014-79-C-0224.

(2) Associate Professor

(3) Research Associate

(4) Professor

SECURITY CLASSIFICATION OF THIS PAGE (When Data Entered)

12 14

REPORT DOCUMENTATION PAGE

READ INSTRUCTIONS BEFORE COMPLETING FORM

1. REPORT NUMBER	2. GOVT ACCESSION NO. AD-A104407
3. RECIPIENT'S CATALOG NUMBER (9)	
4. TITLE (and Subtitle) (6) EDDY CURRENT FLOWS AROUND CRACKS IN THIN PLATES FOR NONDESTRUCTIVE TESTING.	5. TYPE OF REPORT & PERIOD COVERED Topical report. Aug 80 — Mar 81,
	6. PERFORMING ORG. REPORT NUMBER
7. AUTHOR(s) (10) S. Mukherjee, M.A. Morjaria and E.C. Moon	8. CONTRACT OR GRANT NUMBER(s) (15) ONR N00014-79-C-0224
9. PERFORMING ORGANIZATION NAME AND ADDRESS Departments of Structural Engineering and Theoretical and Applied Mechanics, Cornell University, Ithaca, NY 14853	10. PROGRAM ELEMENT, PROJECT, TASK AREA & WORK UNIT NUMBERS NR 064-621
11. CONTROLLING OFFICE NAME AND ADDRESS Office of Naval Research Resident Representative, Room 323, Federal Bldg., 100 State Street, Rochester, NY 14614	12. REPORT DATE (11) 1 Mar 1981
	13. NUMBER OF PAGES 34 pages
14. MONITORING AGENCY NAME & ADDRESS (if different from Controlling Office) Director, Structural Mechanics Program, Material Science Division, Office of Naval Research, Arlington, VA 22217	15. SECURITY CLASS. (of this report) Unclassified
	15a. DECLASSIFICATION/DOWNGRADING SCHEDULE

16. DISTRIBUTION STATEMENT (of this Report)

No restriction

This document has been approved for public release and sale; its distribution is unlimited.

17. DISTRIBUTION STATEMENT (of the abstract entered in Block 20, if different from Report)

18. SUPPLEMENTARY NOTES

19. KEY WORDS (Continue on reverse side if necessary and identify by block number)

Eddy currents, boundary element method, nondestructive testing, magnetomechanics, numerical methods

20. ABSTRACT (Continue on reverse side if necessary and identify by block number)

The boundary element method is used to calculate the induced electric current flow around cracks in thin conducting plates. A low frequency approximation leads to a Poisson equation for the current density potential or stream function. A kernel is used which produces the correct singularity at the crack tip. The boundary condition on the crack, derived from Faraday's law, requires the line integral of the current density around the crack to be zero. Numerical results for induced currents due to a circular induction coil

DD FORM 1 JAN 73 1473 EDITION OF 1 NOV 65 IS OBSOLETE S/N 0102-LF-014-6601

Unclassified

SECURITY CLASSIFICATION OF THIS PAGE (When Data Entered)

403787

Block 20.

are given. These results show that hot spots, due to Joule heating, can occur at the tips of the crack. Comparison of numerical results with infrared scanning experiments of eddy currents in a cracked plate are given. It is hoped that the numerical method presented here will provide a tool to simulate both new and conventional nondestructive eddy current testing techniques.

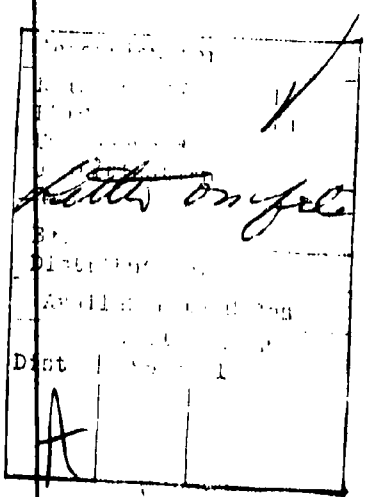

INTRODUCTION

Induced electric currents are generated in conductors by time varying magnetic fields. When the source of the field is outside the body, the induced currents must flow in closed paths, hence the designation "eddy currents". In most problems eddy currents are unwanted since they are a source of heat and energy loss and in some applications can create dynamic forces and magnetic pressures. A few applications, such as magnetic forming and levitation, have exploited the dynamic force producing capability of eddy currents. A third interest in eddy currents is their potential for nondestructive testing. The presence of flaws or cracks interrupt the natural flow of electric current, and the detection of the change of electron flow can give a clue to the presence of flaws in solid conductors.

The calculation of eddy currents in conductors is generally carried out by either using a magnetic or an electric potential. A comparison of the two methods is given by Carpenter [1]. The electric field or current density potential has the advantage that it need be calculated only in the conductor, whereas the magnetic potential must be solved both inside and outside the conductor. The latter method, therefore, poses potential problems for numerical methods.

Numerical methods must generally be used for the solution of eddy current problems in conductors of complex shape. The finite element method (FEM) and the discrete circuit element method have been used for some years for the solution of these problems. Recently, the boundary element method (BEM) (also called the boundary integral equation method) has

been applied to problems in electromagnetics. Wu et al [2] and Ancelle et al [3] have addressed magnetostatic problems by the BEM while Trowbridge [4] has considered magnetostatic problems and eddy current problems by the magnetic potential approach. Very recently, Salon and Schneider [5] have solved problems of eddy current flow in long prismatic conductors by the BEM based on an electric potential approach. The boundary element method has the important advantage that only the boundary of a body (rather than the entire domain) needs to be discretized in a numerical solution procedure - thus effectively reducing the dimension of a problem by one. However, a full matrix must be treated in the BEM while the FEM requires operations on sparse matrices.

The direct boundary element approach [2-5] uses a singular solution of a differential equation in an infinite domain as a kernel in the corresponding integral equation. This direct approach can be used in simply connected as well as multiply-connected domains. However, if a cutout in a conducting plate is a crack, numerical difficulties might arise from discrete modelling of the crack boundary. This difficulty can be overcome if modified kernels are used so that the new kernels are the singular solutions of the governing differential equations for an infinite region with a crack already present in it. This technique has been recently developed for two-dimensional harmonic and biharmonic operators in connection with study of stresses near crack tips in bodies undergoing inelastic deformation [6-8]. Use of these modified kernels allows the proper boundary conditions to be satisfied exactly over the entire crack surface and discretization of the crack surface is no longer necessary in a numerical solution procedure. The method is thus perfectly suited to the study of two-dimensional problems of eddy current flow in cracked bodies.

The purpose of this paper is the study of eddy currents in thin cracked plates with a view towards detection of cracks or flaws by non-destructive testing. An analytical formulation using an electric potential is first presented for the determination of eddy currents in a thin flat conducting plate with a line crack present in it. The applied magnetic field is assumed to be harmonic in time but can have an arbitrary spatial distribution inside the plate. This results in Poisson's equation for the electric potential. A boundary element formulation is next presented using modified kernels for the Laplacian operator in two dimensions.

Numerical results are given for eddy currents in a center-cracked square plate with the applied field being that due to a circular coil. Stream lines are given for various positions of the coil relative to the crack. The induced temperature at any point in the plate is proportional to the square of the density of the induced current at that point. Calculated induced temperature profiles are presented for various coil positions. An eddy current intensity factor, analogous to a stress intensity factor, is defined at a crack tip. Finally, experimental results are presented for an infrared isotherm of induced eddy currents in a cracked aluminum plate.

GOVERNING DIFFERENTIAL EQUATIONS

A thin, flat uniform plate made of a conducting material is shown in Fig. 1. The plate boundary can be arbitrary, its thickness is h and the conductivity of the plate material is σ. The plate has a line crack of length $c = 2a$ present in it. The crack can have arbitrary orientation relative to the outside boundary of the plate.

The coordinate system chosen is shown in Fig. 1. The x_1 and x_2 axes lie on the mid-surface of the plate, with the x_1 axis along the crack and x_2 normal to it. The origin of coordinates lies at the center of the crack in the midsurface of the plate. The x_3 axis is normal to the plate. Also, the unit vectors $\underset{\sim}{i}$, $\underset{\sim}{j}$ and $\underset{\sim}{k}$ are oriented along the coordinate axes.

Consider a current density $\underset{\sim}{J}$, which is induced in the plate by an oscillatory magnetic field $\underset{\sim}{B}^{o}$ outside the plate. The current distribution is assumed to be uniform across the plate thickness and oscillatory in nature. The skin depth, which is inversely proportional to the square root of the frequency, is assumed to be large compared to the plate thickness. Under these assumptions no bending occurs in the plate.

According to Ohm's law

$$\underset{\sim}{J} = \sigma \underset{\sim}{E} \tag{1}$$

where $\underset{\sim}{E}$ is the electric field (the Hall effect or magnetoresistive terms are neglected in Ohm's law).

For low frequency currents, the continuity condition is

$$\underset{\sim}{\nabla} \cdot \underset{\sim}{J} = 0 \tag{2}$$

where $\underset{\sim}{\nabla}$ is the gradient operator in two dimensions. Thus, a stream function (or electric potential) $\psi(x_1, x_2)$ can be defined such that

$$\underset{\sim}{J} = \underset{\sim}{\nabla} \times (\psi \underset{\sim}{k}) = -\underset{\sim}{k} \times \underset{\sim}{\nabla} \psi \tag{3}$$

so that $J_1 = \frac{\partial \psi}{\partial x_2}$, $J_2 = -\frac{\partial \psi}{\partial x_1}$.

Using Faraday's law of induction

$$\nabla \times \underset{\sim}{E} = -\frac{\partial \underset{\sim}{B}}{\partial t} \tag{4}$$

with $\underset{\sim}{B}$ the total magnetic field inside the plate and t time, the governing differential equation for the stream function is

$$\nabla^2 \psi = \sigma \frac{\partial B_3}{\partial t} = \sigma \frac{\partial}{\partial t} (B_3^o + B_3^1) \tag{5}$$

In the above, B_3^1 is the self magnetic field inside the plate due to the current $\underset{\sim}{J}$. In general, this field can be obtained from the Biot-Savart law as an integral, over the plate, of a kernel times the stream function ψ. Equation (5) would then become an integro-differential equation for the stream function [9]. If, however, the applied field is sinusoidal and the resulting skin depth is greater than ten times the plate thickness, the self field term can be neglected relative to the applied field $\underset{\sim}{B}^o$ [10]. Under this assumption, and with $B_3^o = \hat{B}_3^o e^{i\omega t}$ (where $i = \sqrt{-1}$ and ω is the oscillation frequency), the spatial part of the stream function ψ satisfies the equation

$$\nabla^2 \psi = i\omega\sigma \hat{B}_3^o = f(x_1, x_2) \tag{6}$$

which is a two-dimensional Poisson's equation with a prescribed nonhomogeneous term. For simplicity, the same notation is used in the following for the amplitudes of the various oscillatory functions, as has been used so far for the functions themselves.

Eddy current distributions using a similar electric potential approach have been obtained by Salon and Schneider [5]. Their formulation is valid for the determination of currents in long prismatic conductors

and results in a Helmholtz equation for the stream function ψ. Thus, the work of Schneider and Salon is analogous to plane strain problems in mechanics, while the present paper addresses conductors in the shape of thin plates. This is analogous to plane stress.

The current must be tangential to the boundary of the plate at a point on it. Thus, for a point on either the crack boundary ∂C_1 or on the outside boundary ∂C_2 (Fig. 1)

$$\underset{\sim}{J}\cdot\underset{\sim}{n} = \frac{d\psi}{ds} = 0 \tag{7}$$

where $\underset{\sim}{n}$ is an unit normal to the boundary at a point on it and s is the distance measured along a boundary in the anticlockwise sense. Thus, if ψ is a constant a_1 on ∂C_1 and another constant a_2 on ∂C_2, equation (7) is satisfied. One of these constants can be set to zero without loss of generality and the other one is determined by the auxillary condition

$$\oint_{\partial C_1} \underset{\sim}{J}\cdot\underset{\sim}{t}\,ds = 0 \tag{8}$$

where $\underset{\sim}{t}$ is an unit tangent to ∂C_1 at a point on it. Physically, this equation implies that the net flux following through the crack is zero.

The boundary conditions on ψ, in this formulation, are therefore

$$\psi = 0 \quad \text{on the crack boundary } \partial C_1 \tag{9}$$

$$\frac{d\psi}{ds} = 0 \quad \text{on the outside boundary } \partial C_2 \tag{10}$$

$$\oint_{\partial C_1} \frac{d\psi}{dn}\,ds = 0 \tag{11}$$

Equations (9-11) together with the field equation (6) constitute a well posed problem.

It should be noted that this formulation assumes that no current flows across the crack or crack tip. This formulation leads to a current density singularity at the crack tip, as does analogous formulations for the stress at a crack tip. Physically we suspect that there is a finite resistance or current leakage across the crack tip which would relieve the singularity in actual conductors. However this is not considered in this paper. Instead we will characterize the current at the crack tip by a current density intensity factor analogous to that in fracture mechanics.

BOUNDARY ELEMENT FORMULATION

Integral equations

An integral equation formulation for Poisson's equation (6) can be written as (Fig. 1)

$$2\pi\psi(p) = \oint_{\partial C_2} K(p,Q)G(Q)ds_Q + \int_A K(p,q)f(q)dA_q \qquad (12)$$

This is a single layer potential formulation where G, a source strength function on the outside boundary, must be determined from the boundary condition on it (equation 10). The points p (or P) and q (or Q) are source and field points, respectively, with capital letters denoting points on the boundary of the body and lower case letters denoting points inside the body. The area of the body B is denoted by A.

The kernel $K(p,q)$, for a simply connected region, is normally chosen to be a singular solution of Laplace's equation in appropriate dimensions,

eg. $$K = \ell n r_{pq} = \mathrm{Re}[\hat{\phi}(z,z_o)]$$

with $$\hat{\phi}(z,z_o) = \ell n(z-z_o) \quad .$$

Here r_{pq} is the distance between a source point p and a field point q, Re denotes the real part of the complex argument and z and z_o are the source and field points, respectively, in complex notation.

In this problem, however, the kernel must be chosen such that it vanishes on the crack boundary ∂C_1. This is achieved by augmenting $\hat{\phi}$ with a second piece ϕ^* which equals the negative of $\hat{\phi}$ when the source point z lies on ∂C_1 (Fig. 1). Furthermore, ϕ^* must satisfy Laplace's equation and be regular inside the body B. For an elliptical cutout ∂C_1, ϕ^* is derived by making use of the mapping function

$$z = \omega(\xi) = \frac{1}{\xi} + m\xi \tag{13}$$

which transforms the region on and outside an ellipse in the z plane to a region on and inside an unit circle in the ξ plane. The parameter m equals $(a-b)/(a+b)$ (with $(a+b) = 2$) in terms of the semi-major and minor axies, a and b respectively, of the ellipse. For the line crack in this problem, a is taken to be equal to 2 and b is zero. Thus, m equals 1. Using this value of m, the augmented function ϕ is determined as [6]

$$\phi(z,\bar{z},z_o) = \ell n(1-r_1/\xi) - \ell n(1-r_1\bar{\xi}) \tag{14}$$

where $r_i = \frac{z_o \pm \sqrt{z_o^2-4}}{2}$, $|r_i| \leq 1$

$$\xi = \frac{z \pm \sqrt{z^2-4}}{2} \quad , \quad |\xi| \leq 1$$

and the kernel K in equation (12) is

$$K(p,q) = \mathrm{Re}[\phi(z,\bar{z},z_o] \tag{15}$$

A superposed bar denotes, as usual, the complex conjugate of a complex quantity.

Use of K from equation (15) in equation (12) satisfies equation (9). It has been proved in ref. [6] that this formulation also satisfies the integral condition (11) on the crack surface. Thus, the proper boundary conditions on the crack surface are satisfied in an implicit manner and discretization of the crack boundary is not necessary in a numerical solution procedure.

The remaining boundary condition (10) on the outside surface is satisfied by using a differentiated version of (12) and taking the limit as p inside B approaches a point P on ∂C_2. Defining

$$\left.\begin{aligned} H_1 &= \mathrm{Re}\left(\frac{\partial\phi}{\partial x_2}\right) = \mathrm{Im}\left(\frac{\partial\phi}{\partial\bar{z}} - \frac{\partial\phi}{\partial z}\right) \\ H_2 &= -\mathrm{Re}\left(\frac{\partial\phi}{\partial x_1}\right) = -\mathrm{Re}\left(\frac{\partial\phi}{\partial z} + \frac{\partial\phi}{\partial\bar{z}}\right) \end{aligned}\right\} \tag{16}$$

and

$$\frac{dK}{ds} = \mathrm{Re}\left[\frac{d\phi}{ds}\right] = H_i n_i \qquad (i \text{ summed over } 1, 2)$$

where n_i are the components of the unit outward normal to ∂C_2 at some point on it, the boundary conditon (10) becomes

$$0 = \oint_{\partial C_2} H_i(P,Q)n_i(P)G(Q)ds_Q + \int_A H_i(P,q)n_i(P)f(q)dA_q \qquad (17)$$

Equation (17) is valid for a point P on ∂C_2 where it is locally smooth. It can be shown that in this case there is no extra term due to a residue from the limiting process. The boundary integral must be interpreted in the sense of a Cauchy principal value.

The current componenets J_1 and J_2 at a point p inside the body are obtained from equations like (12) with the kernel K replaced by $H_1(p,Q)$ and $H_2(p,Q)$ respectively. As p approaches a point on ∂C_2 it can be shown that

if $\quad 2\pi J_j(p^*) = h_j(p^*)$

then $\quad 2\pi J_j(P^*) = h_j(P^*) + \pi t_j(P^*)G(P^*)$

where p^* is infinitesimally close to P^*, ∂C_2 is locally smooth at P^* and $t_j(P^*)$ are the components of the unit anticlockwise tangent vector to ∂C_2 at P^*. Thus, the residue is zero for the normal component and equals $G(P)/2$ for the tangential component of the current, as a point approaches the outer boundary. The actual current components, of course, remain continuous as a point approaches the boundary.

Discretization of equations and solution strategy

The outer boundary of the body, ∂C_2, is divided into N_2 straight boundary elements using N_b ($N_b = N_2$) boundary nodes and the interior of the body, A, is divided into n_i triangular internal elements. A discretized version of equation (17) is

$$0 = \sum_{N_2} \int_{\Delta s_i} H_i(P_M,Q) n_i(P_M) G(Q) ds_Q$$

$$+ \sum_{n_i} \int_{\Delta A_i} H_i(P_M,q) n_i(P_M) f(q) dA_q \qquad (18)$$

where P_M is the point P where it coincides with a node M at a center of a boundary segment on ∂C_2 and Δs_i and ΔA_i are boundary and internal elements respectively.

A simple numerical scheme is used in which the source strengths G are assumed to be piecewise uniform on each boundary segment with their values to be determined at the nodes which lie at the centers of each segment. The integrals of H_i on boundary elements are evaluated analytically for the singular and by Gaussian quadrature for the regular portions. Nonsingular area integrals of known integrands over triangular internal cells are evaluated by Gaussian quadrature. This integrand becomes singular when the source point lies on the side of or inside of a triangle over which the integral is being evaluated. In fact, the location of an internal source point, in equation (12), can be arbitrary. In any case, for singular integrands, the order of the singularity is $1/r$, r being the distance between the source and field points. The area element, however, is $rd\theta dr$ (in polar coordinates). This form of dA_q is used to change the integrand into a regular function, and then the integral is evaluated appropriately by Gaussian quadrature.

Substitution of the piecewise uniform source strengths into equation (18) and carrying out of the necessary integrations leads to an algebraic system of the type

$$\{0\} = [A]\{G\} + \{d\} \qquad (19)$$

The coefficients of the matrix [A] contain boundary integrals of the kernel. The vector {d} contains contributions from the area integrals and the vector {G} the unknown source strengths at the boundary nodes. The dimension of {G} depends only on the number of boundary elements on ∂C_2 and the internal discretization is necessary only for the evaluation of integrals with known integrands.

Equation (12) for the stream function ψ and analogous equations for the current components J_1 and J_2 are discretized in similar fashion.

The solution strategy is as follows. The matrix [A] and vector {d} in equation (19) are first evaluated by using the appropriate expressions for the kernels and the prescribed function f in equation (6). Equation (9) is solved for the vector {G}. This value of {G} is now used in a discretized version of equation (12) to obtain the values of the stream function ψ at any point p. Finally, the current vector at any point is obtained from equations analogous to (12).

NUMERICAL RESULTS

Field Due to a Circular Induction Coil. A center-cracked square plate with a circular induction coil placed above it is shown in Fig. 2. The square plate is of side L with a center crack of length $c = 2a$. The coordinate system is shown in Figs. 1, 2. The coil is of radius a_o with its center at the point (x_1^o, x_2^o, h_o). The induced field $\underset{\sim}{B}^o$ at a point $q\ (x_1, x_2)$ in the plate, from the Biot-Savart law, is

$$\underset{\sim}{B}^o = \frac{\mu_o I}{4\pi} \oint_{coil} \frac{d\underset{\sim}{s} \times \underset{\sim}{R}}{R^3} \tag{20}$$

where μ_o is the permeability of vacuum, I is the current in the coil, $\underset{\sim}{ds}$ a length element along the coil ($\underset{\sim}{ds} = \underset{\sim}{e}_\phi a_o d\phi$) and

$$-\underset{\sim}{R} = (x_1^o - x_1 + a_o\cos\phi)\underset{\sim}{i} + (x_2^o - x_2 + a_o\sin\phi)\underset{\sim}{j} + h_o\underset{\sim}{k}$$

with $R = |\underset{\sim}{R}|$.

Thus, the function $f(x_1,x_2)$ in equation (6) is

$$f(x_1,x_2) = \frac{i\omega\sigma\mu_o I}{c4\pi}\oint_{coil}\frac{c\underset{\sim}{k}\cdot(\underset{\sim}{ds}\times\underset{\sim}{R})}{R^3} \tag{21}$$

The dimensionless line integral I can be written as

$$\oint_{coil}\frac{\underset{\sim}{k}\cdot(\underset{\sim}{ds}\times\underset{\sim}{R})c}{R^3} = \int_o^{2\pi}\frac{c\{a_o[(x_1^o-x_1)\cos\phi+(x_2^o-x_2)\sin\phi]+a_o^2\}d\phi}{[(x_1^o-x_1)^2+(x_2^o-x_2)^2+2a_o[(x_1^o-x_1)\cos\phi+(x_2^o-x_2)\sin\phi]+a_o^2+h_o^2]^{3/2}}$$

This integral is evaluated by Gaussian integration in the numerical calculations (6 Gauss points between 0 and $\pi/2$).

Nondimensional Equations. Equation (6), with $f(x_1,x_2)$ defined by equation (21), can be nondimensionalized to the form

$$\hat{\nabla}^2\hat{\psi}(\hat{x}_1,\hat{x}_2) = I \tag{22}$$

where $\hat{\psi} = \frac{\psi c}{iIR}$, $\hat{x}_i = 4x_i/c$, $\hat{x}_i^o = 4x_i^o/c$

$(i=1,2)$, $\hat{L} = 4L/c$, $\hat{a}_o = 4a_o/c$, $\hat{h}_o = 4ho/c$

$\hat{\nabla}^2 = \frac{\partial^2}{\partial\hat{x}_1^2} + \frac{\partial^2}{\partial\hat{x}_2^2}$, $R = \frac{16c^2}{2\pi\delta^2}$ and the skin depth

$\delta = \sqrt{\frac{2}{\omega\sigma\mu_o}}$

Further, the dimensionless current density is

$$\hat{J} = \frac{Jc^2}{4iIR}$$

Geometrical Parameters and Boundary Mesh. The values of the geometrical parameters, used in the numerical calculations, are

$$\hat{L} = 20 \quad , \quad \hat{a}_o = 4 \text{ and } 1 \quad , \quad \hat{h}_o = 1 \quad ,$$

$$\hat{x}_1^o = 0, 1, 2, 3, 4, 5, \text{ and } 6 \quad , \quad \hat{x}_2 = 0$$

The dimensionless crack length here is 4. The results for any crack length c can be determined from the above equations.

A typical boundary element mesh for the problem is shown in Fig. 3. Only the upper half of the plate is modelled due to symmetry. This mesh has 42 boundary segments and 128 internal cells. The boundary elements are uniformly distributed along the boundary of the plate. The symmetry line is not discretized. The unknown values of the source strengths G (equation 18) lie only on the boundary nodes. The internal discretization is necessary only for the evaluation of the area integral in equation (18). The integrand in this integral is completely known. Nonsingular integrals are evaluated by Gaussian quadrature with 6 Gauss points on a boundary segment and 7 Gauss points in an internal cell. A 4×4 grid is used for the evaluation of singular area integrals (see below equation (18)).

The uniform field problem is analogous to the Saint Venant problem of torsion of long prismatic bars with end couples. The computer program used here has been verified by solving torsion problems in the absence of cracks [11] and the logic for inclusion of the crack has been verified by solving Mode III crack problems [6].

The boundary integral algorithm was also applied to a plate with a notch cut instead of a crack. The results were compared with an analysis using a finite element method, [10], and the agreement was very good.

Eddy Current and Temperature Lines. Eddy current stream lines (constant $\hat{\psi}$ lines) are shown in Figs. 4-5 for a coil of radius 4. Fig. 4 shows the lines in a plate without a crack in it, and Fig. 5 shows how the stream lines are affected by the crack for different coil positions. A close-up of the stream lines near a crack tip for $\hat{x}_1^o = 2$ is shown in Fig. 6. The crowding of stream lines near the crack tip leads to large gradients of $\hat{\psi}$ (and therefore large induced currents) in this region. The local temperature is proportional to the square of the current density $(\hat{J}\cdot\hat{J})$ and this leads to a hot spot at the crack tip. This is shown in Fig. 7 which shows lines of constant induced temperature. The contour lines go off scale as one approaches the crack tip. The behavior of the singularity at the crack tip is discussed later in the subsection entitled 'Eddy Current Intensity Factor'.

Finally, the stream lines for a smaller coil (of diameter equal to half the crack length) centered at (2,0,1) are shown in Fig. 8.

Temperature Scans. A matter of considerable interest in this approach to nondestructive testing is the existence of hot spots due to the presence of a crack. Figure 9 shows calculated temperature profiles along a line slightly above the crack $(\hat{x}_2=0.05)$ for different coil positions $(\hat{x}_1^o =$ 0,1,2 and 6). The coil radius here is four (equal to the crack length). Hot spots are seen near the crack tips. The strongest hot spots arise when an edge of the coil is near a crack tip. These temperatures are much higher than other moderate hot spots elsewhere in the plate. A discussion of experimental results is given in the next section.

Self Induced Field at Center of Coil. One method of electromagnetic non-destructive testing uses one or more passive sensing coils together with an active induction coil [12]. The purpose of the sensing coils is to measure the self induced field (back e.m.f.) and to try to observe changes in back e.m.f. due to the presence of cracks. With this in view, the self induced field was calculated at the center of the induction coil for various coil positions. The method used is the Biot-Savart Law which gives the induced field B_3^I as

$$B_3^I = \frac{\mu_o h}{4\pi} \int_{\text{plate}} \underset{\sim}{k} \cdot \frac{(\underset{\sim}{J} \times \underset{\sim}{R})}{R^3} \, dA \tag{23}$$

where now the induced current density in the plate, must be used. The integral must be evaluated over the plate with dA an area element in the plate. The current density is assumed to be piecewise uniform over each internal cell in this approximate calculation, with the value determined at the centroid (x_1^c, x_2^c) of the cell. Thus, in this case

$$\underset{\sim}{R} = (x_1^o - x_1^c)\bar{i} + (x_2^o - x_2^c)\bar{j} + h_o\bar{k}$$

and

$$B_3^I = \frac{\mu_o h}{4\pi} \sum_{i=1}^{n_i} \frac{\Delta A_i [J_1(x_2^o - x_2^c) - J_2(x_1^o - x_1^c)]}{R^3} \tag{24}$$

where ΔA_i is the area of the i_{th} triangular element.

A plot of normalized B_3^I with respect to coil position is shown in Fig. 10. The values are normalized with respect to B_3^I when the coil center is directly above the crack center (i.e. $x_1^o = x_2^o = 0$). It is seen that in this example the position of the coil relative to the crack causes little variation in the induced field at the coil center. From

these calculations, it appears that for low frequencies the back e.m.f. method is not useful for detection of cracks and that the temperature scan approach appears to be much more promising for nondestructive testing in this case.

Eddy Current Intensity Factor. It is well known from elastic fracture mechanics that stress components exhibit a square root singularity near a crack tip. It is therefore expected that the components of the current vector, in this problem, should display similar behavior near a crack tip. This, in fact, is the case, as shown in Fig. 11 where $\hat{J}^2$ is plotted as a function of $\hat{r}$, the distance from the right crack tip. The plot is for the coil center at (1,0,1). The eddy current density squared is seen to be inversely proportional to the distance r.

An eddy current intensity factor M_{III}, analogous to the stress intensity factor for Mode III, is defined here as

$$\hat{J}^2 = M_{III} \frac{c}{r} \tag{25}$$

A plot of M_{III} at the two crack tips, as functions of coil position, is shown in Fig. 12. The eddy current intensity factor is seen to peak when an edge of the coil is near a crack tip.

Computing Times. All the computing reported in this paper was carried out on an IBM 370/168 computer at Cornell University. A typical computing time for stream lines in a cracked plate for a fixed coil position (eg. Fig. 8) was 100 c.p.u. seconds.

EXPERIMENTAL RESULTS

Infrared Experiments

Conventional eddy current nondestructive techniques use a small induction coil and search coils to induce eddy currents near the surface of solids and to measure to back emf generated by these currents [12]. To detct a flow or crack, the coils must be moved over the surface near the flow in order to measure a change in voltage in the search coil. Recently a new method has been proposed using infrared scanning technology [10]. This method is based on the fact that eddy currents create heat and that this small temperature change can be detected using an infrared sensitive device.

In the present experiments an aluminum plate 15 cm x 30 cm, 0.51 mm thick, had a crack placed in its center, parallel to the 15 cm width. The crack was created by scoring a line in the aluminum with a sharp edge and flexing the plate until fatigue produced a thorough crack in the plate. The length of the crack was 6 cm. One tip of the crack was 3 cm from one edge of the plate and the other was 6 cm from the other edge.

The induction coil was wound from 10 turns of copper wire on a 5.1 cm coil form so that the mean diameter of the coil was about 5.7 cm, slightly smaller than the crack length. The width of the coil was 1.3 cm and the coil face was placed 6.4 mm from the plane of the cracked plate.

Pulsed electric currents of the order of 9.3 KA peak current and 3.2 msec. duration were used with a rise time to peak of about 0.7 msec. The sensitivity of the infrared system was 0.1 - 0.2°C. If an infrared scan is made of the plate immediately after the firing of the current pulse, heat conduction may be neglected, and the measured rise in temperature is proportional to the integral of J^2 over time. (See e.g. [10].)

The infrared system used for these experiments is a UTI Corp. Spectrotherm infrared scanning system. Radiation from different points in

the plane of focus is detected by a photoconductive crystal. A two-dimensional scan is obtained by two sets of rotating mirrors. The output can be displayed either on a grey scale tube or the voltage can be color quantized into ten colors. Figure 13 shows a black and white photograph of two color quantized infrared scans. Each of the scans represent J^2 "isotherms" for different induction coil positions. The top photo corresponds to a coil position centered at the middle of the crack. The bottom photo corresponds to an induction coil position centered to the left of the crack with the coil center 4 cm from the left edge of the plate. These photos show that a "hot" spot forms at the tip of the crack due to the current flowing around the crack. (The white line shows the vertical position of the crack.) In Figure 13 a right crack tip shows up as circular isotherms. When the coil position is moved to the left the left crack tip shows up as a hot spot, which appear as circular isotherms. The hot spot on the left edge is due to increase of current density near the edge. Needless to say, the color photographs are more dramatic. But the experiments show the same qualitative behavior as the numerical results in Figures 7, 9, 14 and 15.

Of course further experimental work must be done to establish the practical use of this technique, especially as regards below-surface cracks that do not penetrate the solid. The results do indicate the potential for such a technique. It is a visual method whose features change qualitatively as well as quantitatively when a crack interupts the flow of induced currents.

ACKNOWLEDGMENTS

This research was supported by the Office of Naval Research, Washington, DC under Contract Number N00014-79-C-0224, Task number NR064-621 with Cornell University. The assistance of Mr. K. Hara with the infrared experiments is acknowledged.

REFERENCES

1. Carpenter, C.J., "Comparison of Alternative Formulations of Three-Dimensional Magnetic Field and Eddy Current Problems at Power Frequencies," Proceedings of the IEE, Vol. 124, No. 11, Nov. 1977, pp. 66-74.

2. Wu, Y.S., Rizzo, F.J., Shippy, D.J., and Wagner, J.A., "An Advanced Boundary Integral Equation Method for Two-Dimensional Electromagnetic Field Problems," Electric Machines and Electromechanics, Vol. 1, 1977, pp. 301-313.

3. Ancelle, B., and Sabonnadiere, J.C., "Numerical Solution of 3D Magnetic Field Problems using Boundary Integral Equations," IEEE Transactions on Magnetics, Proceedings of INTERMAG, Sept. 1980.

4. Trowbridge, C.W., "Applications of Integral Equation Methods for the Numerical Solution of Magnetostatic and Eddy Current Problems". Report No. RL-76-071, Rutherford Laboratory, Chilton, Didcot, England. June 1976.

5. Salon, S.J. and Schneider, J.M., "A Comparison of Boundary Integral and Finite Element Formulations of the Eddy Current Problem," IEEE Paper 80 SM 526-4, 1980.

6. Mukherjee, S. and Morjaria, M., "Boundary Element Analysis of Time-Dependent Inelastic Deformation of Cracked Plates Loaded in Anti-plane Shear". International Journal of Solids and Structures. (In Press).

7. Mukherjee, S. and Morjaria, M., "A Boundary Element Formulation for Planar, Time-dependent Inelastic Deformation of Plates with Cutouts," International Journal of Solids and Structures, Vol. 17, No. 1, Jan. 1981, pp. 115-126.

8. Morjaria, M. and Mukherjee, S., "Numerical Analysis of Planar Time-dependent Inelastic Deformation of Plates with Cracks by the Boundary Element Method," International Journal of Solids and Structures, Vol. 17, No. 1, Jan. 1981, pp. 127-143.

9. Moon, F.C., "Problems in Magneto-solid Mechanics," Chapter 5 in Mechanics Today, Vol. 4, (S. Nemat-Nasser, ed.), Pergamon Press, Oxford, 1978, pp. 307-390.

10. Yuan, K.Y., Moon, F.C. and Abel, J.F., "Numerical Solutions for Coupled Magnetomechanics", Department of Structural Engineering Report Number 80-5, Departments of Structural Engineering and Theoretical and Applied Mechanics, Cornell University, February 1, 1980. See also, "Magnetic Forces in Plates Using Finite Elements", Proceedings of the Third Engineering Mechanics Division Speciality Conference, ASCE, Austin, Texas, September 1979, pp. 730-733.

11. Mukherjee, S. and Morjaria, M., "Comparison of Boundary Element and Finite Element Methods in the Inelastic Torsion of Prismatic Shafts". International Journal for Numerical Methods in Engineering (In Press).

12. Libby, H.L., Introduction to Electromagnetic Nondestructive Test Methods. Wiley-Interscience, New York, 1971.

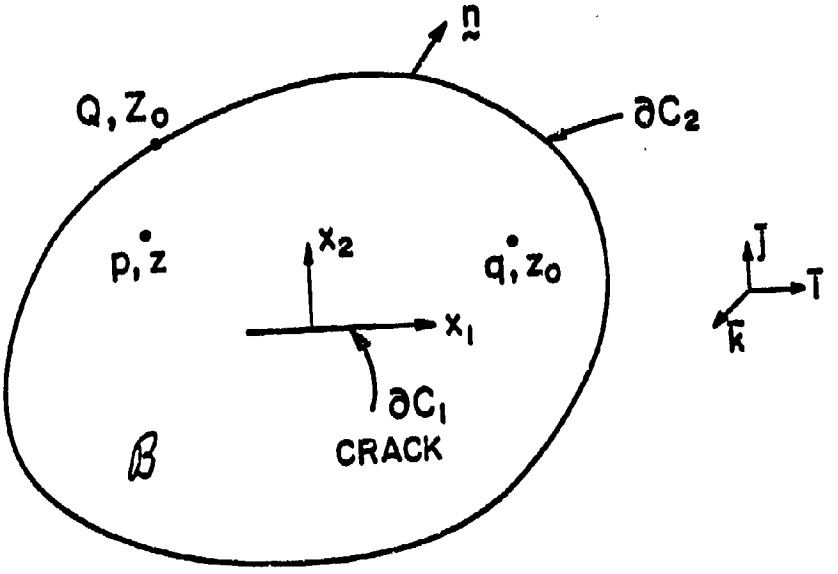

Figure 1. Cracked plate.

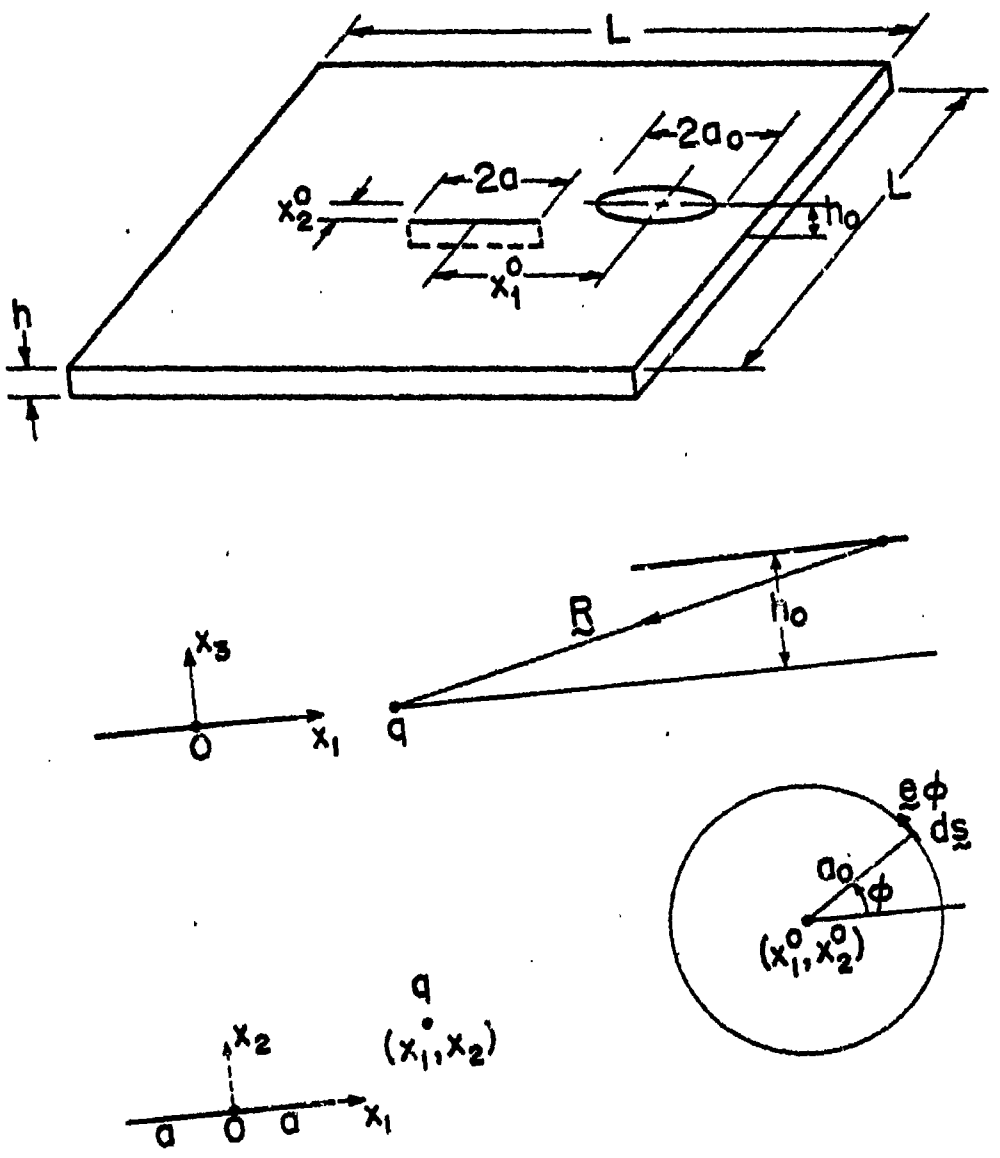

Figure 2. Diagram showing coil and cracked plate geometry.

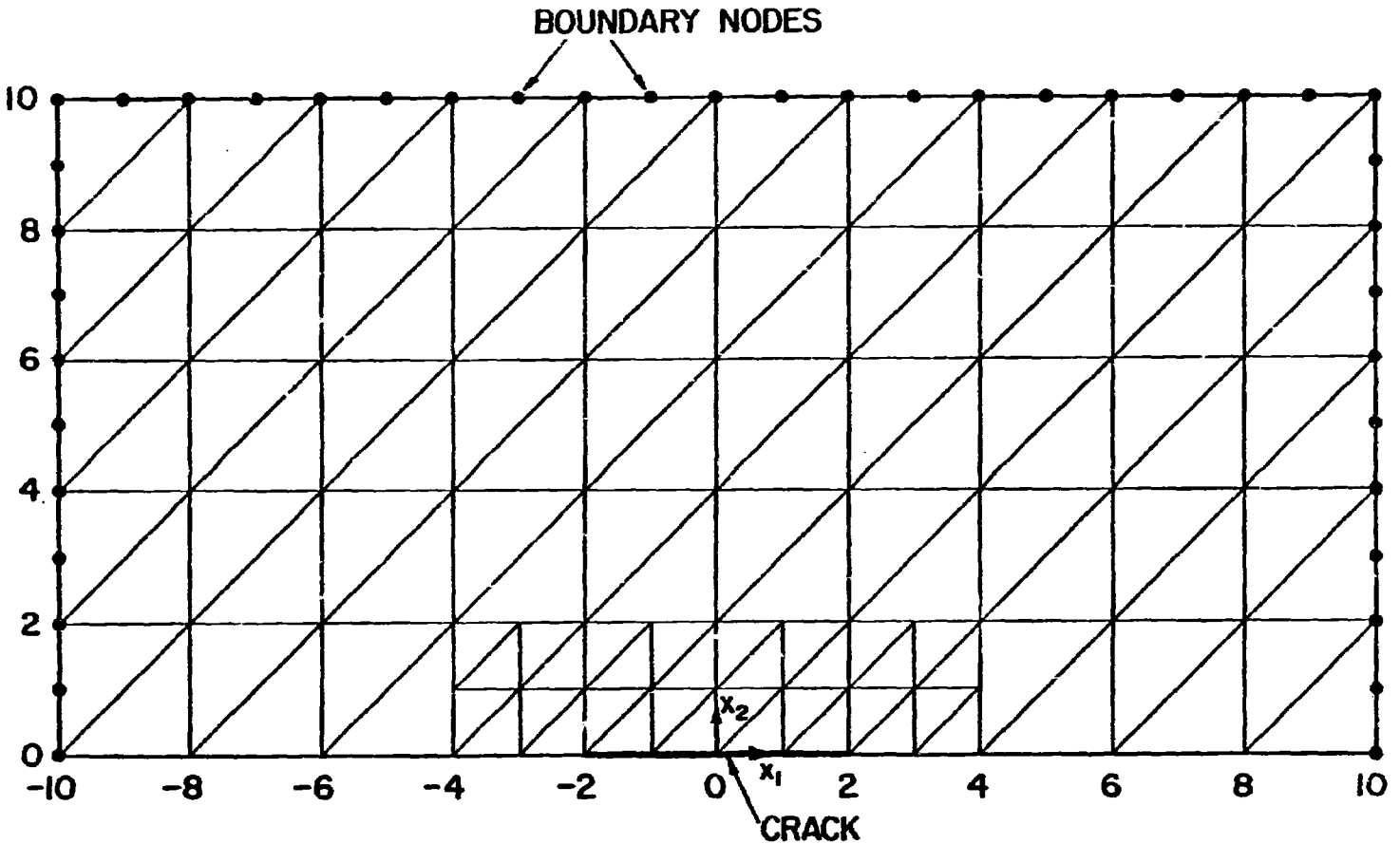

Figure 3. Typical boundary element mesh.

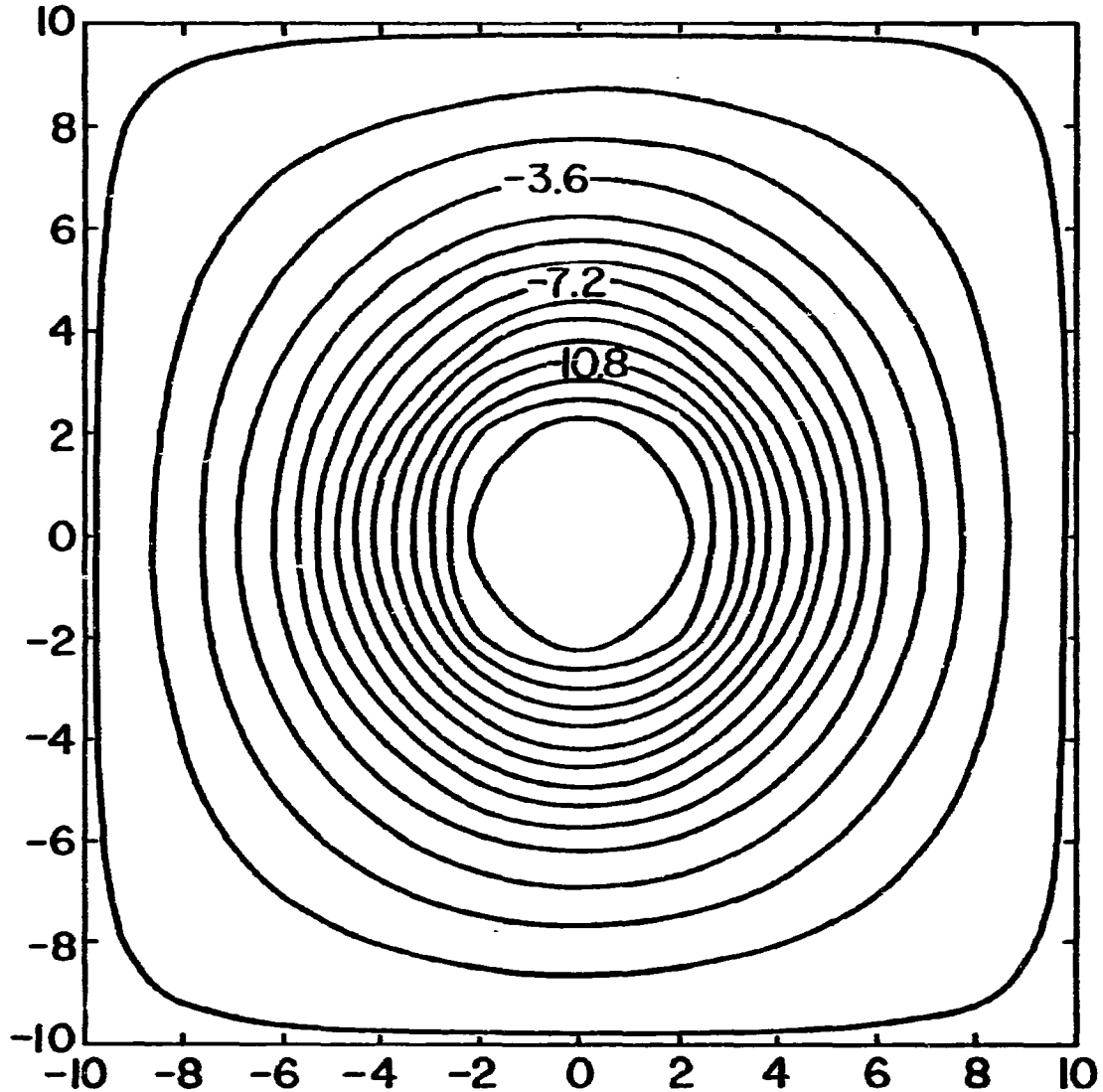

Figure 4. Stream lines for induced currents in an uncracked square plate by a circular coil. $\hat{L} = 20$, $\hat{a}_o = 4$, $\hat{x}_1^o = \hat{x}_2^o = 0$, $\hat{h}_o = 1$.

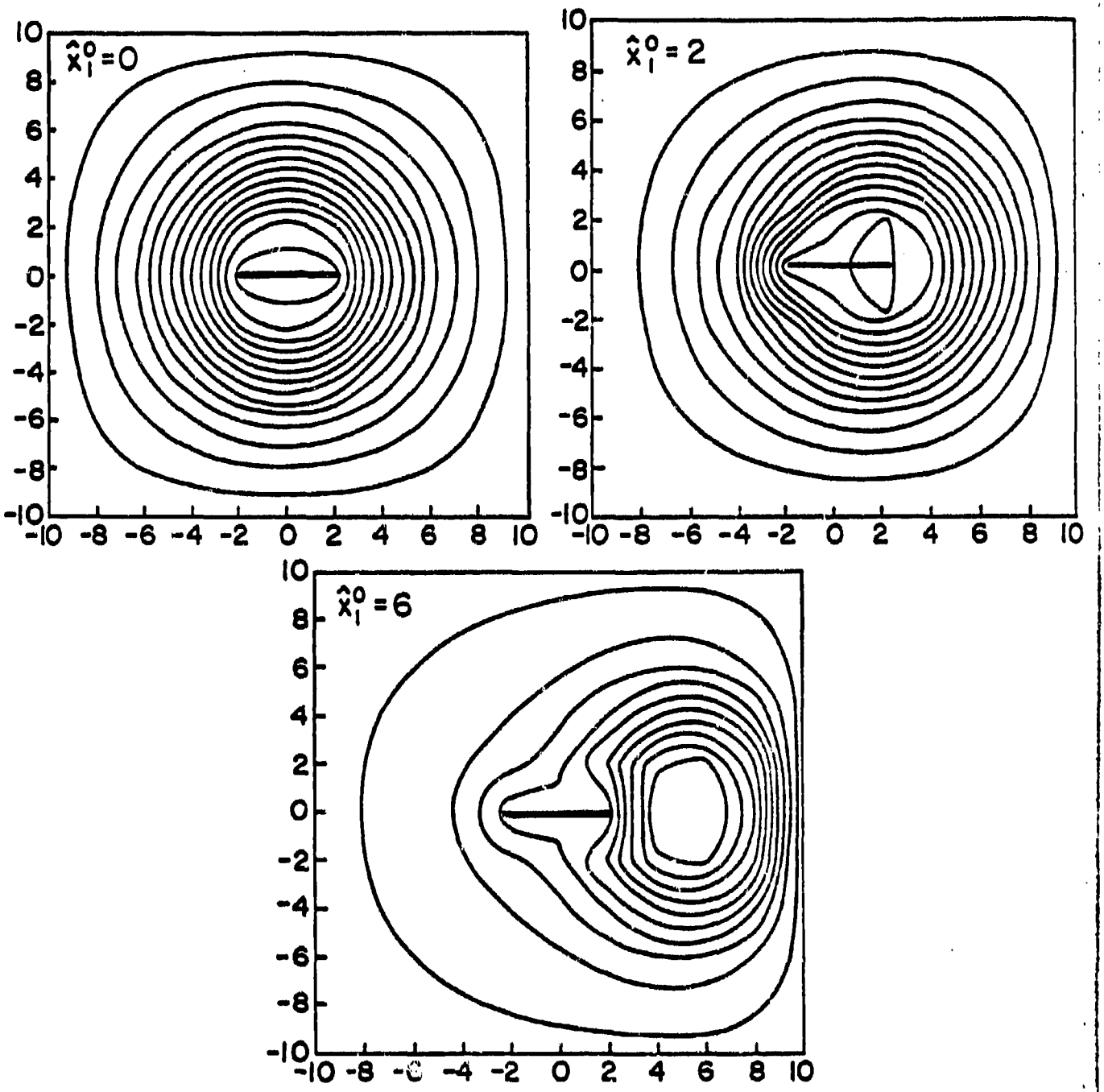

Figure 5. Stream lines for induced currents in a cracked square plate by a circular coil for various coil positions. $\hat{L} = 20$, $\hat{a}_o = 4$, $\hat{x}_2^o = 0$, $\hat{h}_o = 1$.

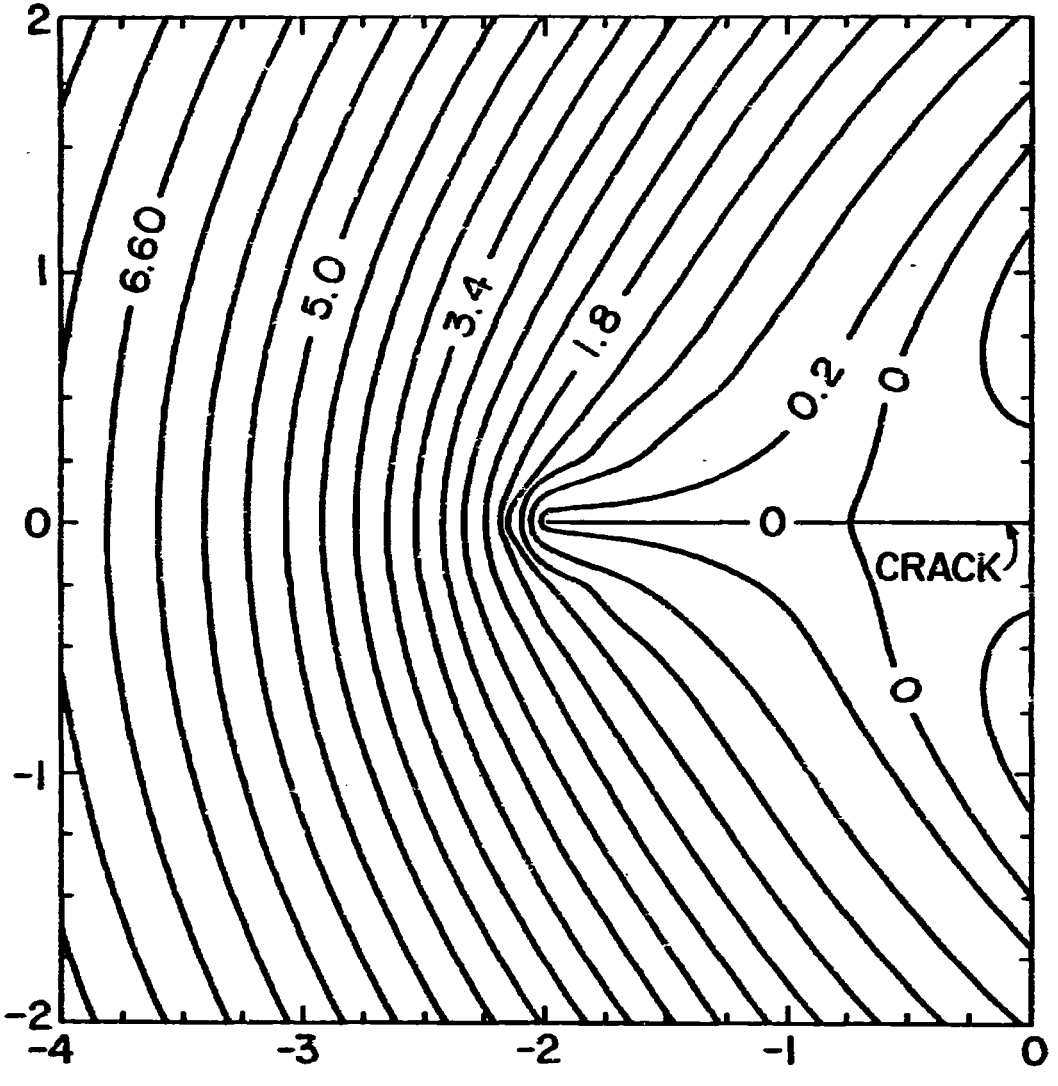

Figure 6. Eddy current stream lines around the tip of a crack. $\hat{a}_o = 4$, $\hat{x}_1^o = 2$, $\hat{x}_2^o = 0$, $\hat{h}_o = 1$.

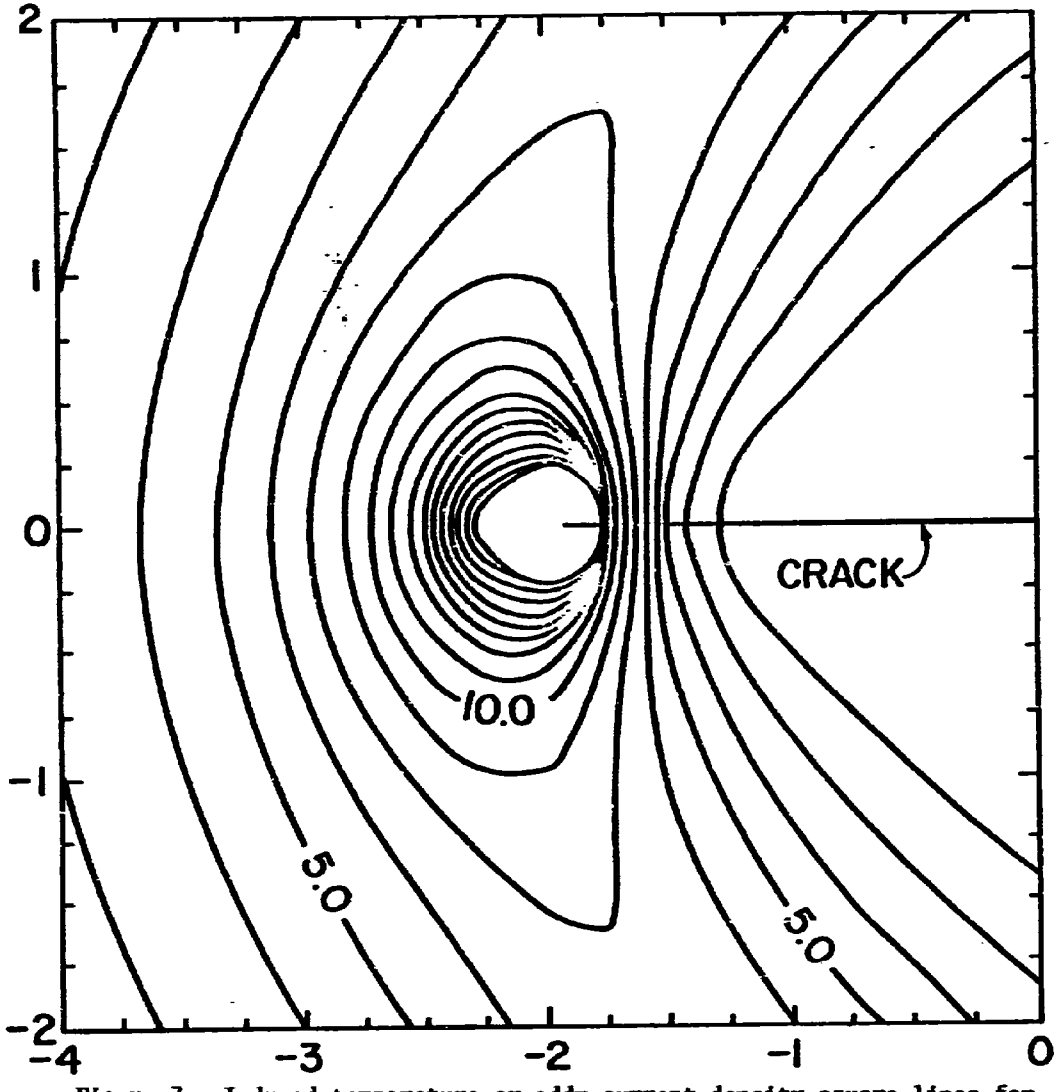

Figure 7. Induced temperature or eddy current density square lines for induced currents in a cracked plate by a circular coil. $\hat{a}_o = 4$, $\hat{x}_1^o = 2$, $\hat{x}_2^o = 0$, $\hat{h}_o = 1$.

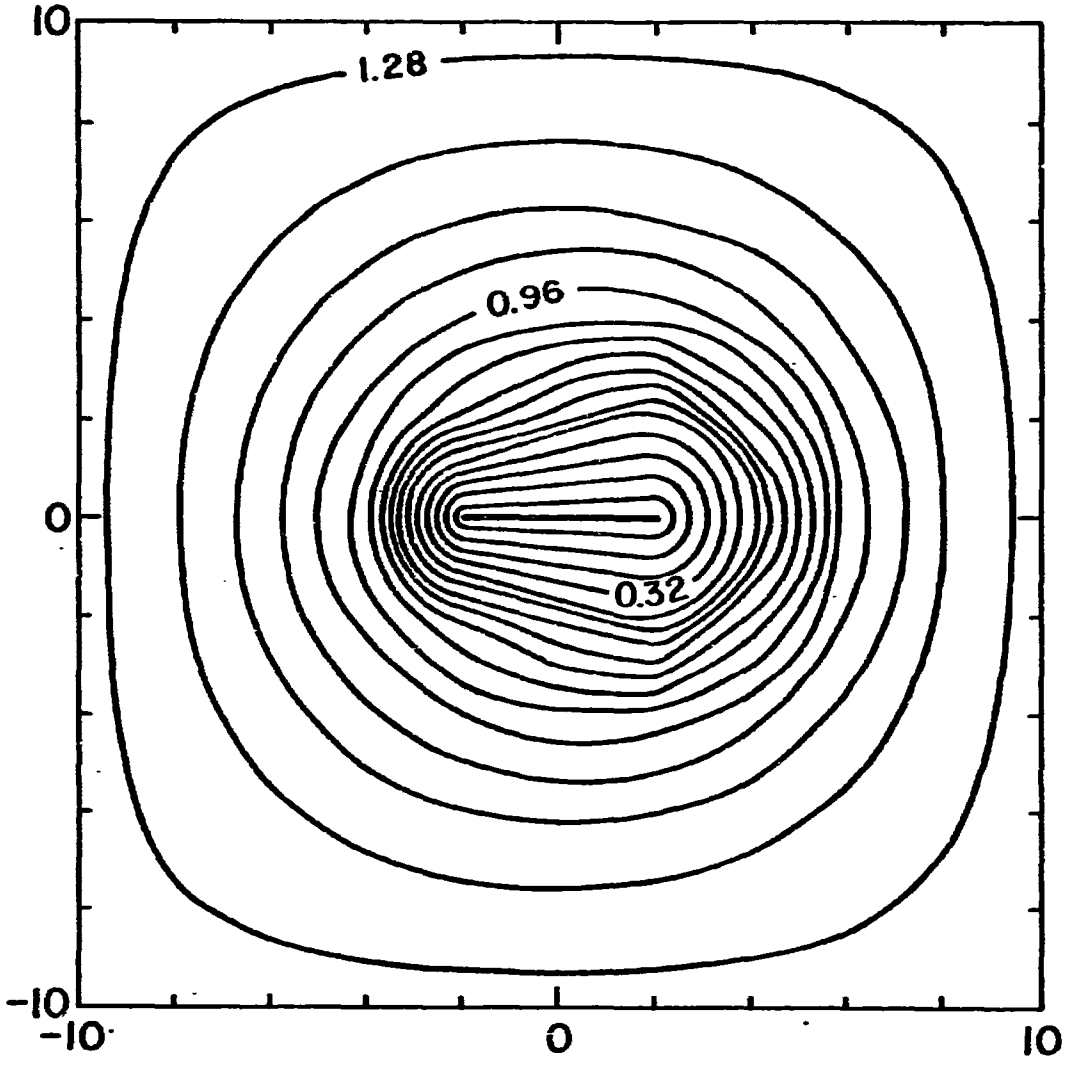

Figure 8. Stream lines for induced currents in a cracked square plate by a circular coil. $\hat{a}_o = 1$, $\hat{x}_1^o = 2$, $\hat{x}_2^o = 0$, $\hat{h}_o = 1$.

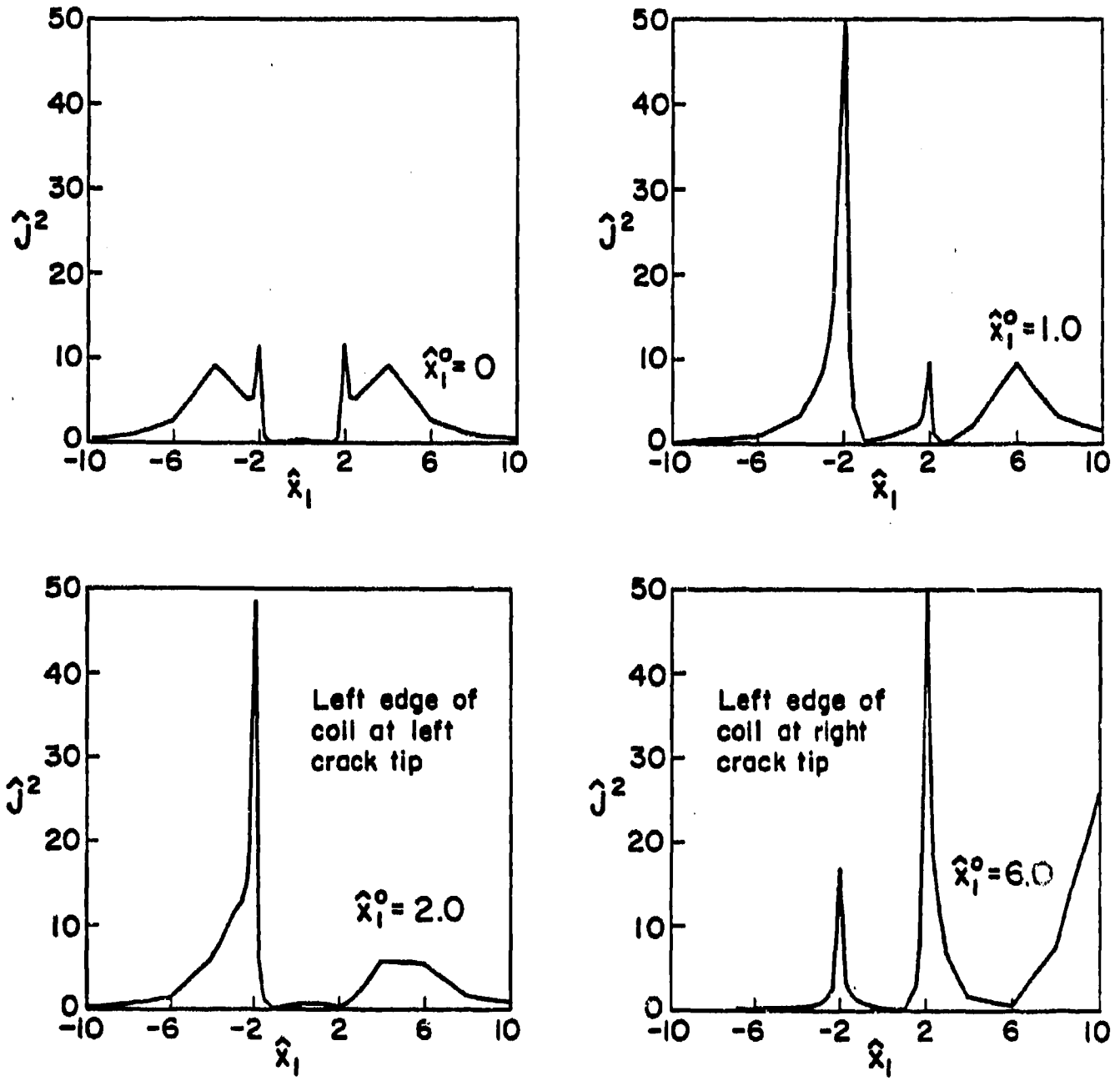

Figure 9. Plots of induced temperature or eddy current density squared along a line slightly above the crack ($\hat{x}_2 = 0.05$) for various coil positions. $\hat{a}_o = 4$, $\hat{x}_2^o = 0$, $\hat{h}_o = 1$.

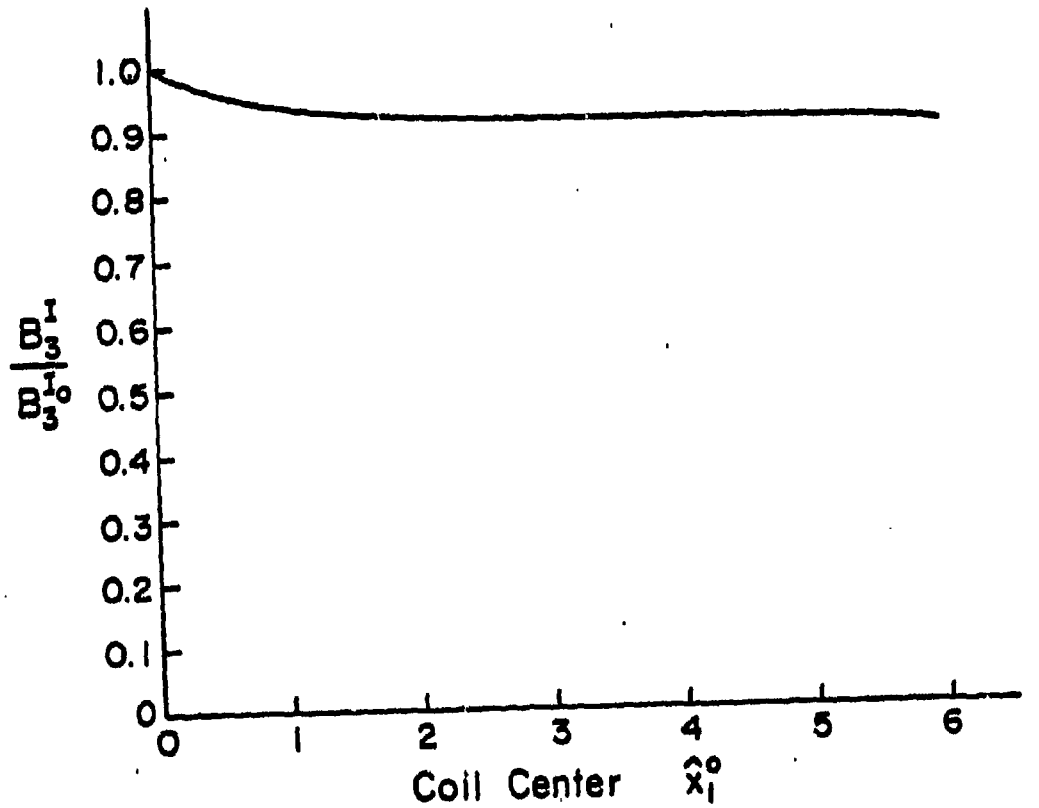

Figure 10. Self induced field at the center of the induction coil as a function of coil position. $\hat{a}_o = 4$, $\hat{x}_2^o = 0$, $\hat{h}_o = 1$.

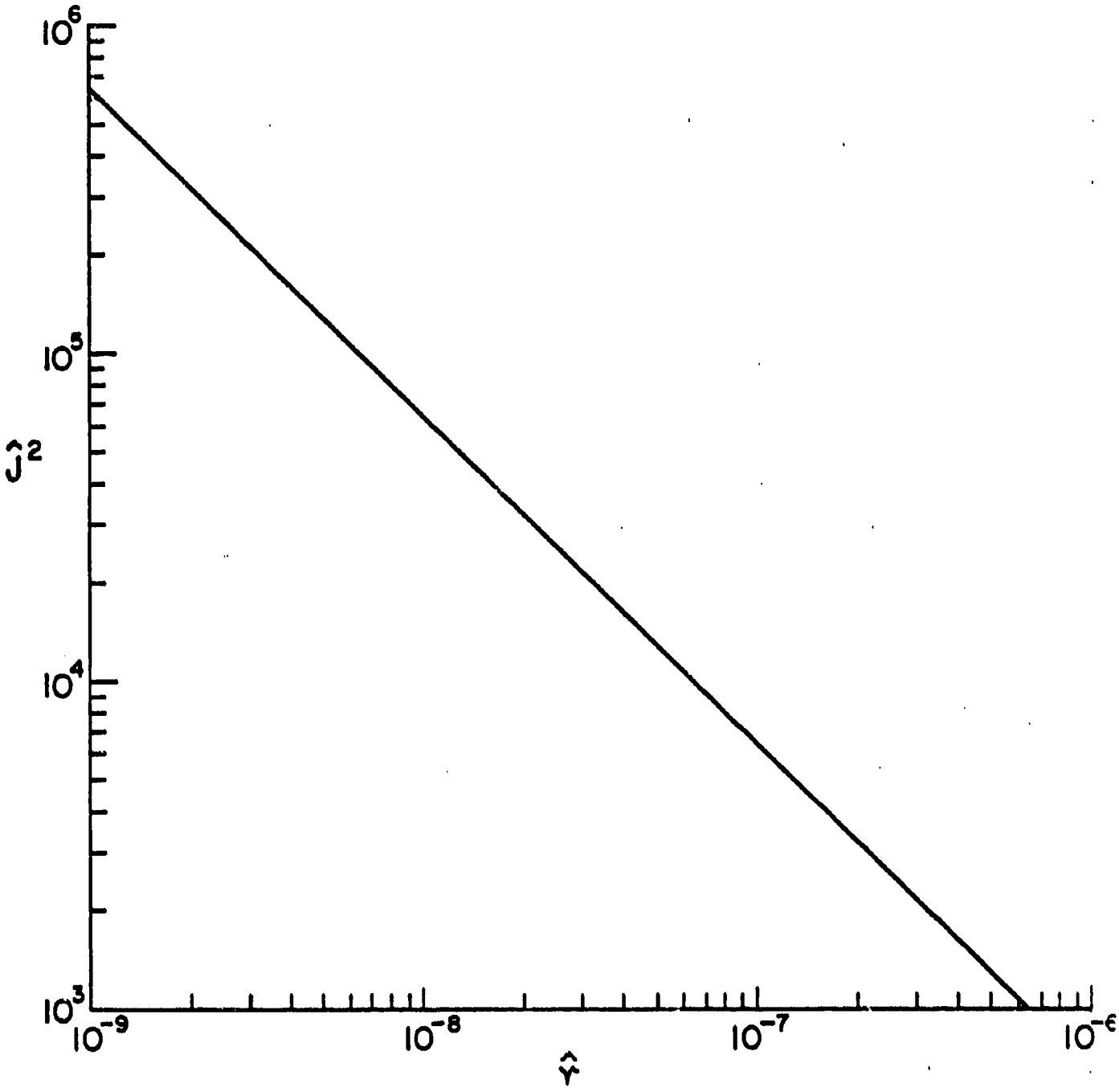

Figure 11. Induced eddy current density squared as a function of position near the right crack tip ($\hat{x}_1 = 2$). $\hat{a}_o = 4$, $\hat{x}_1^o = 1$, $\hat{x}_2^o = 0$, $\hat{h}_o = 1$.

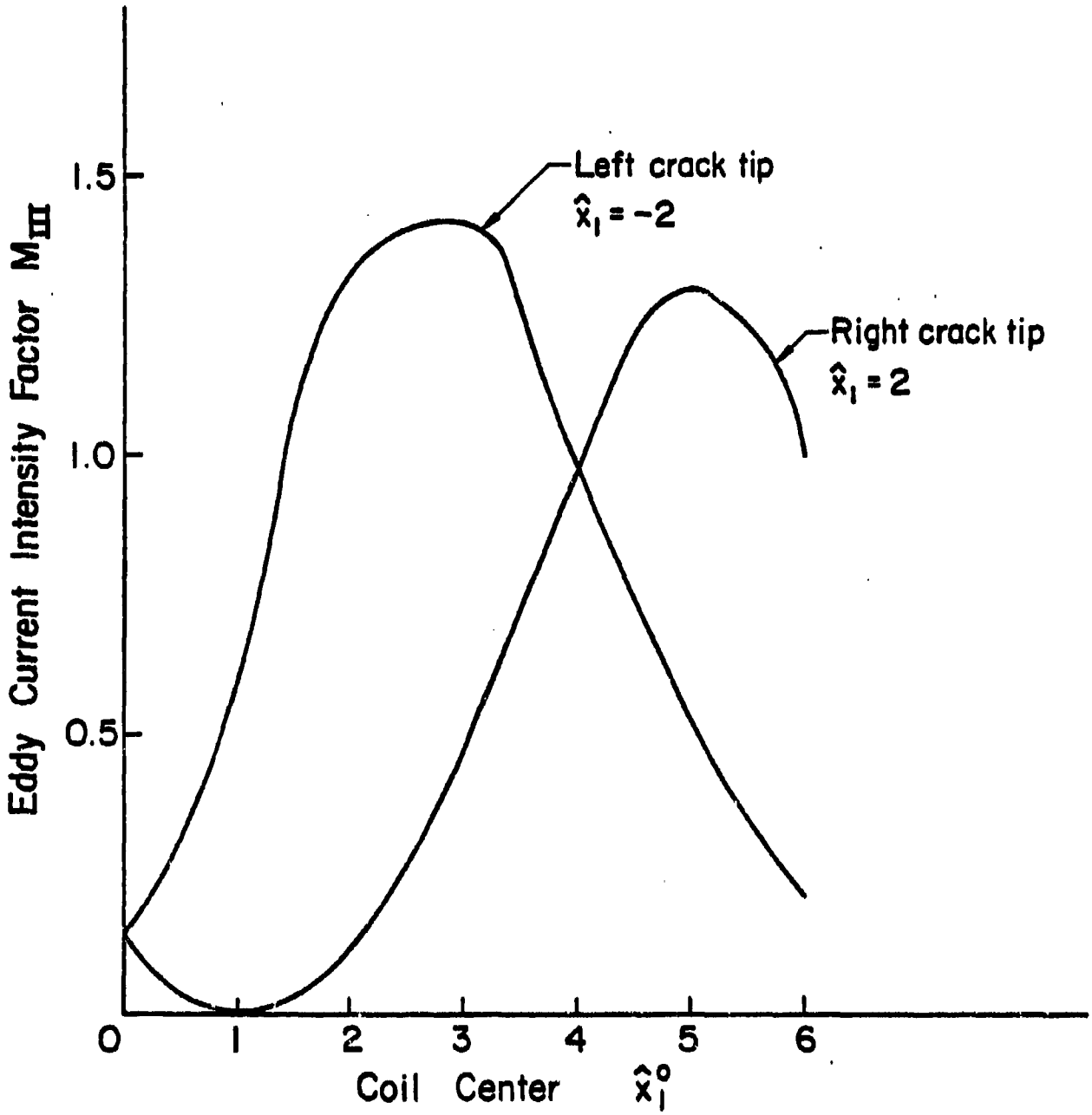

Figure 12. Eddy current intensity factor at crack tips as functions of coil position. $\hat{a}_o = 4$, $\hat{x}_2^o = 0$, $\hat{h}_o = 1$.

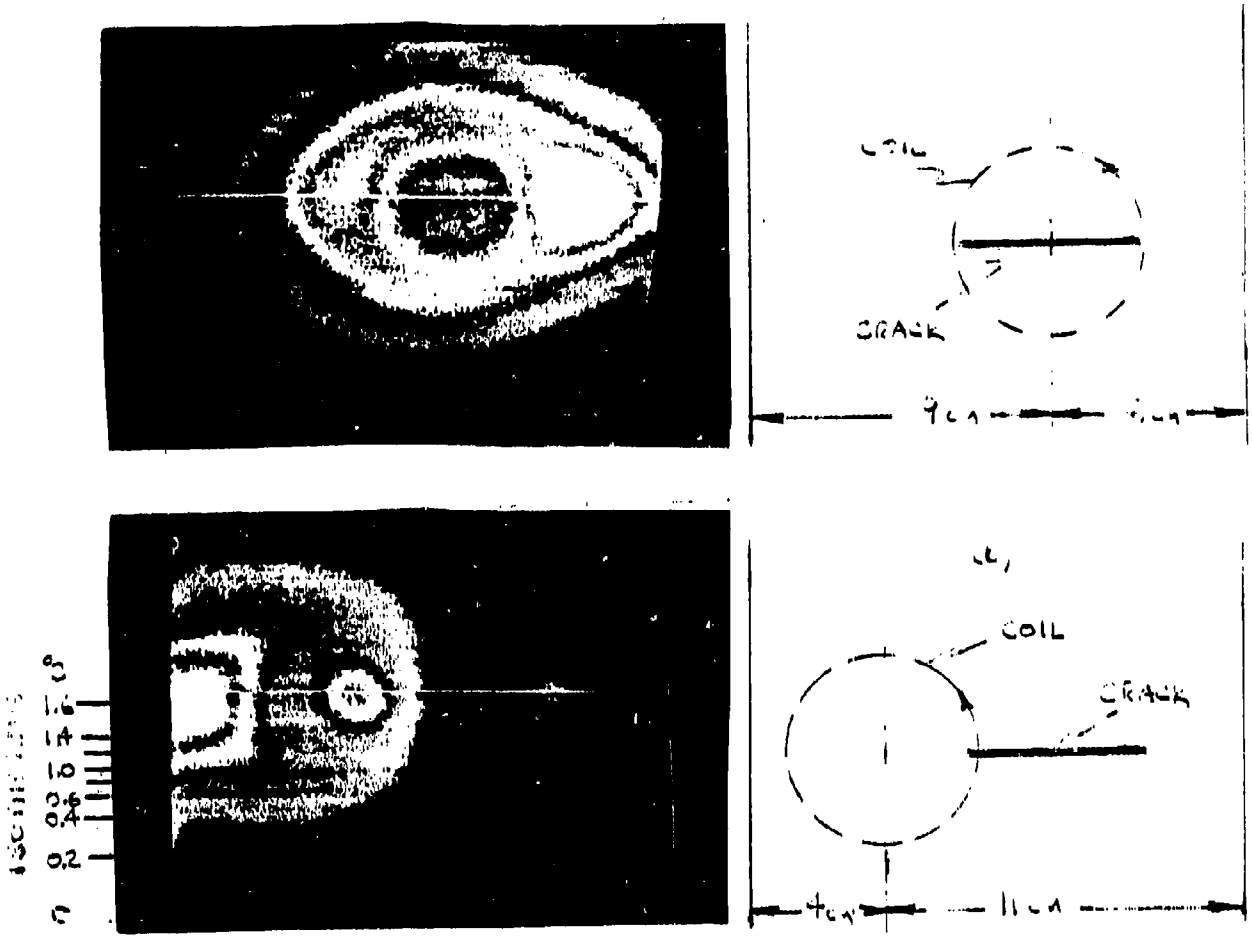

Figure 13. Black and white photographs of color quantized infrared isotherms of induced eddy currents in a cracked aluminum plate.

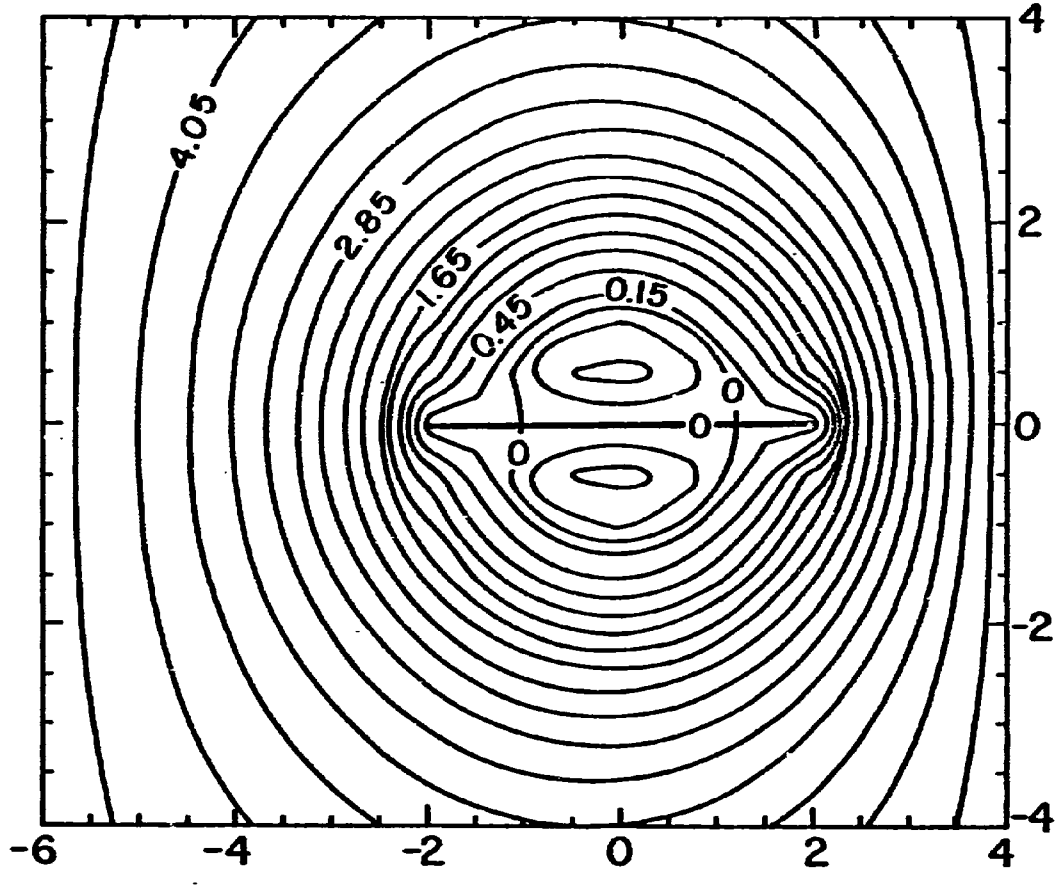

Figure 14. Calculated stream lines for induced currents in a cracked square plate by a circular coil for the experimental situation (Fig. 13a) with $\hat{a}_o = 1.91$, $\hat{x}_1^o = \hat{x}_2^o = 0$, $\hat{h}_o = 0.85$.

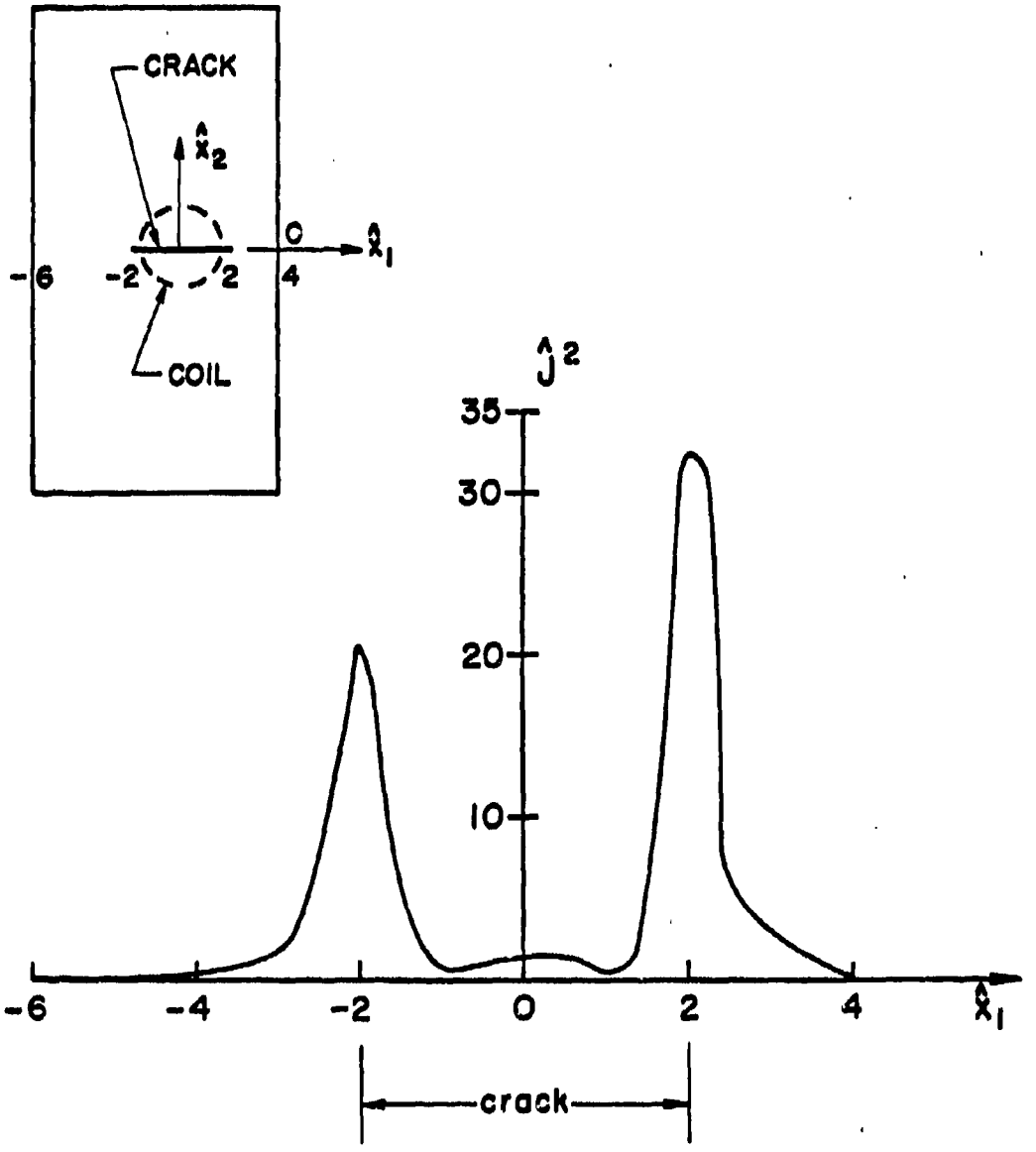

Figure 15. Calculated induced temperature (or eddy current density squared) along a line slightly above the crack ($\hat{x}_2 = 0.05$) for the experimental situation (Fig. 13a) with $\hat{a}_o = 1.91$, $\hat{x}_1^o = \hat{x}_2^o = 0$, $\hat{h}_o = 0.85$.